Langmuir
Article
pubs.acs.org/Langmuir

Synthesis of Magnetic/Luminescent Alginate-Templated Composite Microparticles with Temperature-Dependent Photoluminescence under High-Frequency Magnetic Field

Jiwei Liu,[†,‡] Yu Zhang,*[,†] Changzhi Yan,[†] Chunyu Wang,[†,‡] Ruizhi Xu,[†] and Ning Gu*[,†]

[†]*State Key Laboratory of Bioelectronics; Jiangsu Key Laboratory for Biomaterials and Devices, Southeast University, Nanjing 210096, P. R. China, and* [‡]*School of Chemistry and Chemical Engineering, Southeast University, Nanjing 210096, P. R. China*

Received July 23, 2010. Revised Manuscript Received October 6, 2010

Highly magnetic luminescent alginate-templated composite microparticles were successfully synthesized by a novel process combining emulsification and layer-by-layer self-assembly techniques. The composite microparticles were characterized by ζ-potential analyzer, transmission electron microscope, X-ray diffraction, Fourier transform infrared spectroscope, fluorescence spectrophotometer, and vibrating sample magnetometer. Experimental observations indicated that the composite microparticles had excellent magnetic properties, and its photoluminescence could be precisely controlled by varying the number of deposition cycles of polyelectrolytes and CdTe/polyelectrolyte multilayers. Moreover, the composite microparticles could be heated up in a high-frequency magnetic field and demonstrated linear temperature-dependent photoluminescence over the range from room temperature to hyperthermia temperature. The composite microparticles are expected to be promising candidates for biomedical applications, such as immunoassay, biosensing and imaging, and cancer diagnosis and treatment.

Introduction

Iron oxide magnetic nanoparticles (MNPs), e.g., Fe_3O_4 or γ-Fe_2O_3, are of great interest due to their excellent superparamagnetism and ease of synthesis and have been extensively investigated in biomedical fields, including cell separation,[1,2] magnetic resonance imaging,[3,4] drug delivery systems,[5] and hyperthermia.[6] Semiconductor nanocrystals, or quantum dots (QDs), have gained increasing attention in technological applications and fundamental studies due to their unique properties such as small size, high quantum yield, and excellent photostability. The QDs exhibit size-dependent tunable photoluminescence (PL) with narrow emission bands that can be precisely tuned from blue to the near-infrared by varying the QD size and components as well as broad absorption spectra that allow the simultaneous excitation of different QDs at a single wavelength.[7−10] Also, they demonstrate temperature-dependent emission characteristics and have been employed as optical temperature probes.[11−13] Such advantages superior to conventional organic dyes make QDs very attractive for a broad range of biomedical applications.

Over the past decade, great efforts have been made to incorporate the MNPs and QDs in a single entity that enjoys both the advantages of MNPs and QDs and offers highly potential applications such as magnetic bioseparation and magnetic resonance imaging simultaneously coupled with fluorescence immunoassays and imaging. Yi et al.[14] and Kim et al.[15] simultaneously encapsulated both MNPs and QDs in a silica shell to prepare magnetic luminescent composite particles by employing the sol−gel method. However, the distance between the MNPs and QDs was too close to be controlled, leading to a strong interaction between the MNPs and QDs, which would dramatically diminish the PL of the composite particles. Liu et al.[16] synthesized multifunctional $CdSe/SiO_2/Fe_3O_4$ composite particles driven by the electrostatic interactions. The particles have favorable saturation magnetization (Ms) and the PL intensity will increase with the thickness of silica shell. Recently, magnetic luminescent composite particles were constructed by the layer-by-layer (LbL) self-assembly technique.[17,18] Nevertheless, the literature about the synthesis of composite particles with excellent Ms and PL is still scarce.

In this paper, a novel process combining emulsification and LbL self-assembly techniques was employed to synthesize magnetic

*To whom correspondence should be addressed. E-mail: guning@seu.edu.cn (N.G.), zhangyu@seu.edu.cn (Y.Z.). Phone: +86-25-83794960. Fax: +86-25-83792576.

(1) Berry, C. C.; Wells, S.; Charles, S.; Curtis, A. S. G. *Biomaterials* **2003**, *24*, 4551–4557.
(2) Smith, J. E.; Medley, C. D.; Tang, Z. W.; Shangguan, D.; Lofton, C.; Tan, W. H. *Anal. Chem.* **2007**, *79*, 3075–3082.
(3) Kim, D. K.; Zhang, Y.; Kehr, J.; Klason, T.; Bjelke, B.; Muhammed, M. *J. Magn. Magn. Mater.* **2001**, *225*, 256–261.
(4) Lee, H.; Lee, E.; Kim, D. K.; Jang, N. K.; Jeong, Y. Y.; Jon, S. *J. Am. Chem. Soc.* **2006**, *128*, 7383–7389.
(5) Neuberger, T.; Schopf, B.; Hofmann, H.; Hofmann, M.; von Rechenberg, B. *J. Magn. Magn. Mater.* **2005**, *293*, 483–496.
(6) Jordan, A.; Scholz, R.; Wust, P.; Schirra, H.; Schiestel, T.; Schmidt, H.; Felix, R. *J. Magn. Magn. Mater.* **1999**, *194*, 185–196.
(7) Michalet, X.; Pinaud, F.; Lacoste, T. D.; Dahan, M.; Bruchez, M. P.; Alivisatos, A. P.; Weiss, S. *Single Mol.* **2001**, *2*, 261–276.
(8) Sargent, E. H. *Adv. Mater.* **2005**, *17*, 515–522.
(9) Bakalova, R.; Zhelev, Z.; Aoki, I.; Kanno, I. *Nature Photonics* **2007**, *1*, 487–489.
(10) Yan, J. L.; Estevez, M. C.; Smith, J. E.; Wang, K. M.; He, X. X.; Wang, L.; Tan, W. H. *Nano Today* **2007**, *2*, 44–50.
(11) Wang, S. P.; Westcott, S.; Chen, W. *J. Phys. Chem. B* **2002**, *106*, 11203–11209.
(12) Labeau, O.; Tamarat, P.; Lounis, B. *Phys. Rev. Lett.* **2003**, *90*, 2574041–2574044.
(13) Liu, T. C.; Huang, Z. L.; Wang, H. Q.; Wang, J. H.; Li, X. Q.; Zhao, Y. D.; Luo, Q. M. *Anal. Chim. Acta* **2006**, *559*, 120–123.
(14) Yi, D. K.; Selvan, S. T.; Lee, S. S.; Papaefthymiou, G. C.; Kundaliya, D.; Ying, J. Y. *J. Am. Chem. Soc.* **2005**, *127*, 4990–4991.
(15) Kim, J.; Lee, J. E.; Lee, J.; Yu, J. H.; Kim, B. C.; An, K.; Hwang, Y.; Shin, C. H.; Park, J. G.; Kim, J.; Hyeon, T. *J. Am. Chem. Soc.* **2006**, *128*, 688–689.
(16) Liu, B.; Xie, W. X.; Wang, D. P.; Huang, W. H.; Yu, M. J.; Yao, A. H. *Mater. Lett.* **2008**, *62*, 3014–3017.
(17) Hong, X.; Li, J.; Wang, M. J.; Xu, J. J.; Guo, W.; Li, J. H.; Bai, Y. B.; Li, T. J. *Chem. Mater.* **2004**, *16*, 4022–4027.
(18) Salgueirino-Maceira, V.; Correa-Duarte, M. A.; Spasova, M.; Liz-Marzan, L. M.; Farle, M. *Adv. Funct. Mater.* **2006**, *16*, 509–514.

luminescent composite microparticles. The process could be divided into two steps. First, magnetic alginate microspheres were prepared via the emulsification technique. Second, the as-synthesized magnetic alginate microspheres were used as templates for the deposition of polyelectrolytes and CdTe QDs via the LbL self-assembly technique. The reason to use the alginate was that it was a well-known naturally occurring polysaccharide because of its unique properties including a relatively inert hydrogel environment within the matrix and a mild room-temperature encapsulation process.[19] It is well-known that the LbL self-assembly technique is based on electrostatic attraction between the oppositely charged species deposited. Since alginate contains carboxylate groups on both polyguluronate and polymannuronate units, alginate microspheres exhibit negative surface charge, allowing them to be used as negatively charged templates for polyelectrolyte LbL self-assembly.[20] Therefore, two kinds of magnetic luminescent composite microparticles were obtained by varying the number of deposition cycles of polyelectrolytes and CdTe/polyelectrolyte multilayers. The resulting composite microparticles had excellent magnetic properties and its PL could be precisely controlled by the LbL self-assembly technique. To the best of our knowledge, the temperature-dependent PL under a high-frequency magnetic field (HFMF), which is important to temperature monitoring during hyperthermia treatment, has not been previously reported. The as-synthesized composite microparticles could be heated up in the HFMF, and its temperature-dependent PL was investigated at moderate temperature over the range from room temperature to hyperthermia temperature. It is believed that the composite microparticles described here could serve both as magnetic materials for hyperthermia and as optical temperature probes for temperature monitoring during the hyperthermia treatment.

Experimental Section

Materials. Sodium alginate (1 wt %, viscosity ≥0.2 Pa·s, 20 °C), sorbitan trioleate (SPAN 85), polyoxyethylene sorbitan trioleate (TWEEN 85), isooctane, acetone, ferric chloride hexahydrate, ferrous sulfate heptahydrate, ammonia solution, sodium hydroxide, calcium chloride, and cadmium chloride were all purchased from Shanghai Chemicals Co. Ltd. *meso*-2,3-Dimercaptosuccinic acid (DMSA), 3-mercaptopropionic acid (MPA), sodium poly(styrenesulfonate) (PSS, $M_w \sim 70$ kDa), and poly(allylamine hydrochloride) (PAH, $M_w \sim 70$ kDa) were obtained from Sigma-Aldrich. All chemicals were of analytical reagent grade and used as received. Milli-Q water (18.2 MΩ·cm^{-1}) was used in all experiments.

Preparation of Magnetic Alginate Microspheres (MAMs). The preparation of magnetic alginate microspheres has been reported previously.[21,22] Briefly, 50 g of aqueous solution of DMSA-coated γ-Fe_2O_3 MNPs (200 mg) and sodium alginate (500 mg) was dispersed in 75 g of isooctane containing 3.392 g of SPAN 85, ultrasonicating (250 W) and stirring (1200 rpm) for 10 min. Then, a solution of 5 g of isooctane containing 1.808 g of TWEEN 85 was added to the emulsion under stirring and ultrasonication at the same power for 20 min. After that, another 30 min of stirring was proceeded to achieve a stable water-in-oil emulsion droplet. Subsequently, the droplets were ionically cross-linked by addition of 20 mL of an aqueous solution containing 10 wt % of calcium chloride. Finally, the products were washed with water by magnetic decantation four times and redispersed into water.

Scheme 1. Illustration of the LbL Process Forming the Alginate-Templated Composite Microparticles

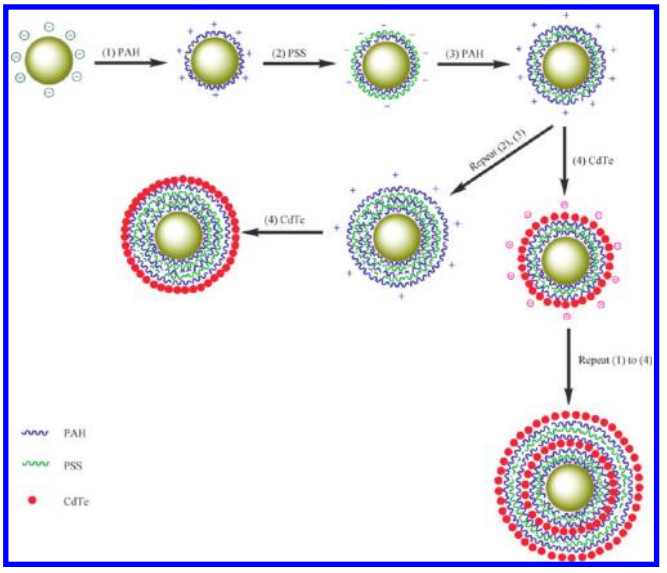

Fabrication of MPA-Capped CdTe QDs. Highly luminescent CdTe QDs were fabricated in an aqueous system with a novel Te source to conveniently produce a CdTe precursor using a cathodic stripping Te electrode.[23,24] Typically, the generation of CdTe precursors was carried out using an applied potential of −1.2 V in the electrolyte containing 2.0 mM $CdCl_2$ and 16.6 μL of MPA at pH 10 adjusted with 0.1 M NaOH solution. The CdTe precursors could be easily formed, accompanied by a color change of electrolyte from colorless to dark brown. The amount of the CdTe precursor was controlled by adjusting the charge consumed during cathodic stripping according to Faraday's law. Subsequently, the solution of CdTe precursors was heated in a water bath with moderate stirring for 20 h at 80 °C. Finally, the products were deposited by acetone, and after centrifugation the precipitate was washed by acetone at least three times and redispersed into water.

Synthesis of Alginate-Templated Composite Microparticles. Two kinds of alginate-templated composite microparticles (MAMs/PE_n/CdTe, MAMs/$(PE_3$/CdTe$)_n$) were synthesized via the LbL self-assembly technique,[17,20,22,25] as illustrated in Scheme 1. For MAMs/PE_n/CdTe, 2 mL of positively charged PAH (4 mg/mL in water containing 0.1 M $CaCl_2$) was added into 200 μL of MAMs suspension. Deposition was allowed to proceed for 20 min under shaking, after which the suspension was washed with water by magnetic decantation to remove excess polyelectrolyte. Then, negatively charged PSS (4 mg/mL in water containing 0.1 M $CaCl_2$) was deposited in the same conditions and procedures. The above processes were repeated until the desired number of PAH/PSS/PAH multilayers was formed. Subsequently, 1 mL of the MPA-capped CdTe QDs was added to 2 mL of PE_n-coated MAMs solution with an outermost layer of positively charged PAH. The adsorption was allowed to proceed for 30 min under shaking. Finally, the composite microparticles were washed with water by magnetic decantation three times and redispersed into water. For MAMs/$(PE_3$/CdTe$)_n$, the primer three polyelectrolyte layers (PAH/PSS/PAH, PE_3) were deposited prior to the deposition of the CdTe QDs layer, as described above. After each deposition step, the excess polyelectrolyte was removed by three repeated magnetic decantation/washing/redispersion cycles. Then, the CdTe QDs was deposited

(19) Gombotz, W. R.; Wee, S. F. *Adv. Drug Delivery Rev.* **1998**, *31*, 267–285.
(20) Zhu, H. G.; Srivastava, R.; McShane, M. J. *Biomacromolecules* **2005**, *6*, 2221–2228.
(21) Liu, J. W.; Zhang, Y.; Chen, D.; Yang, T.; Chen, Z. P.; Pan, S. Y.; Gu, N. *Colloids Surf., A* **2009**, *341*, 33–39.
(22) Liu, J. W.; Zhang, Y.; Wang, C. Y.; Xu, R. Z.; Chen, Z. P.; Gu, N. *J. Phys. Chem. C* **2010**, *114*, 7673–7679.
(23) Ge, C. W.; Xu, M.; Liu, J.; Lei, J. P.; Ju, H. X. *Chem. Commun.* **2008**, 450–452.
(24) Liu, J. W.; Zhang, Y.; Ge, C. W.; Jin, Y. L.; Hu, S. L.; Gu, N. *Chin. Chem. Lett.* **2009**, *20*, 977–980.
(25) Zhu, H. G.; Srivastava, R.; Brown, J. Q.; McShane, M. J. *Bioconjugate Chem.* **2005**, *16*, 1451–1458.

by adding 1 mL of the MPA-capped CdTe QDs into 2 mL of PE_3-coated MAMs suspension and subsequently depositing another PE_3 layer, as outlined above for the primer layers. The processes were repeated until the desired number of CdTe QDs was obtained.

Characterization. The size and morphology of the products were characterized by transmission electron microscope (TEM, JEOL, JEM-2100). The samples were prepared by dropping 6 μL of solution on the carbon-coated copper grids and allowing the solution to dry in the air. The surface charge of the products was investigated through a ζ-potential analyzer (Beckman Coulter, Delsa 440SX). Powder X-ray diffraction (XRD, Rigaku, D/MaxRA, $\lambda = 1.5405 \times 10^{-10}$ m, Cu Kα) was used to determined the crystal structure of the products. Infrared spectra were recorded using a Fourier transform infrared spectroscope (FTIR, Nicolet 750), and the samples were pressed as KBr pellets. UV−vis absorption spectra were acquired using an UV−vis−NIR spectrophotometer (UV-3150, Shimadzu) with a scan speed of 200 nm/min. Fluorescence spectra were measured on fluorescence spectrophotometer (Hitachi, F-7000). The samples were contained in a 1 cm quartz cuvette and illuminated with a Xe lamp. Magnetic properties were determined with vibrating sample magnetometer (VSM, LakeShore 7407) at room temperature in a field up to 5 kOe.

A detection system containing the Navitar Zoom6000 system, a SENTech STC-N63 CCD camera, a high-frequency magnetic field (HFMF, 50 kHz), and a fiber-optic thermometry device (FISO Technologies Corp., accuracy ±0.3°) was designed to investigate the temperature-dependent PL of the composite microparticles, as illustrated in Figure S1 in the Supporting Information. It should be noted that a nonmetallic object lens (Sharpscope Precision Corp., magnitude 12×) was used in this detection system to avoid inductive heating of the object lens under the HFMF. To prepare samples for PL measurements, 1 mL of aqueous solution of the composite microparticles with a γ-Fe_2O_3 concentration of 1.67 mg mL^{-1} was mixed with 2 mL of 1% agarose solution and cooled down to form a cylindrical composite. The cylindrical composite was then located in a three-loop copper coil and illuminated with an ac/dc halogen light source. When the power was switched on, the ac magnetic field was produced and the composite was heated up. The optical fiber was inserted into the cylindrical composite to detect temperature changes. The PL intensity photographs were recorded by the CCD camera, and the scanned PL intensity distribution was carried out by software ImageJ.

Results and Discussion

ζ-Potential. The LbL assembly processes were monitored by ζ-potential measurements. As shown in Figure 1a, the original MAMs had a negative ζ-potential of −46.1 mV, and the surface potential of the microparticles was observed to change regularly from +18 mV for PAH to −31 mV for PSS. Further polyelectrolyte depositions caused the ζ-potential to alternate in sign, depending on whether the outermost layer was positively or negatively charged. With driving of the electrostatic interactions, positively charged PAH and negatively charged PSS were alternatively deposited onto the surface of the MAMs, providing a positively charged outer surface to facilitate the adsorption of the negatively charged MPA-capped CdTe QDs. Adsorption of the CdTe QDs onto PE_n-coated MAMs with the outermost layer of positively charged PAH caused the ζ-potential to be −23 mV. Again, MAMs/$(PE_3/CdTe)_n$ were prepared by repetitious deposition of PE_3/CdTe on the MAMs. Figure 1b shows the ζ-potential as a function of repetitiously adsorbed PE_3/CdTe onto the surface of the MAMs. The primer ζ-potential of the $(PE_3/CdTe)_1$ was negative. After deposition of another PE_3 layer, it inversed to be positive. Subsequent adsorption of the MPA-capped CdTe QDs onto PE_3-coated MAMs would result in a negative ζ-potential. The alternation in ζ-potential quantitatively demonstrated a successful deposition of each

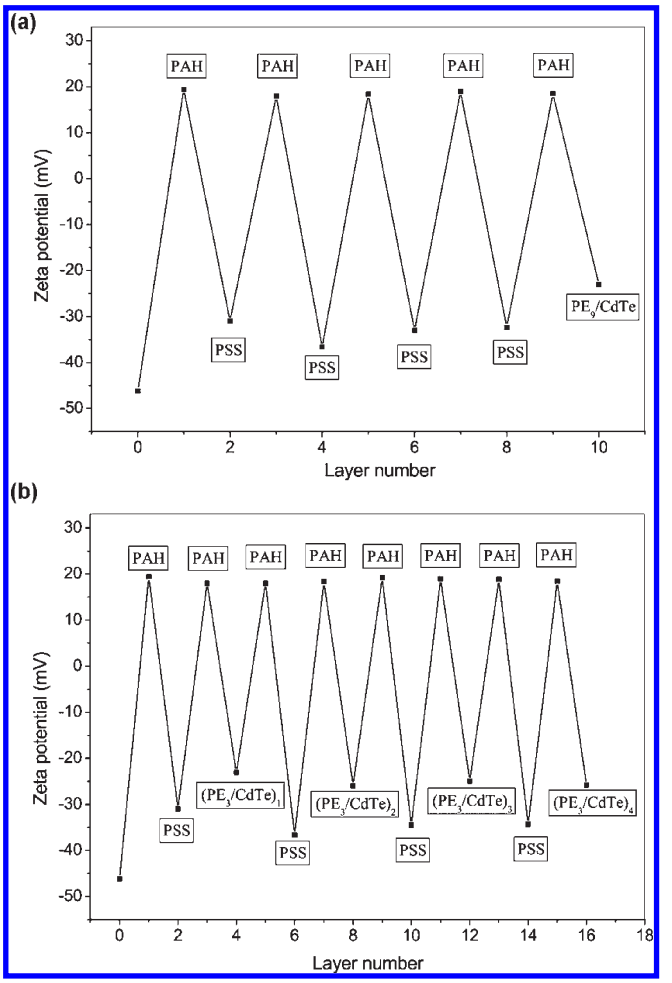

Figure 1. ζ-potentials of (a) MAMs/PE_n/CdTe and (b) MAMs/$(PE_3/CdTe)_n$ as a function of polyelectrolyte layer and CdTe QDs depositions.

polyelectrolyte layer and CdTe QDs onto the surface of the MAMs during the synthesis of the alginate-templated composite microparticles.

TEM. The size and morphology of the as-synthesized products were characterized by TEM. Figure 2a shows the TEM image of the DMSA-coated γ-Fe_2O_3 MNPs, which were used as magnetic cores to synthesize the MAMs. The γ-Fe_2O_3 MNPs were approximately spherical with an average diameter of 18 nm. Figure 2b presents the TEM image of the MPA-capped CdTe QDs with an average size of 3.5 nm, which could also be estimated from its corresponding excitonic absorption peaks[26] (see Figure S2 in the Supporting Information). TEM image of the MAMs revealed that the average diameter of the microspheres was about 860 nm (Figure 2c). Figure 2d shows the TEM image of MAMs/$(PE_3/CdTe)_2$. It could be clearly seen that the composite microparticles displayed a higher surface roughness compared with the MAMs. This is probably due to the deposited polyelectrolyte multilayers and CdTe QDs. Moreover, a TEM image of an individual composite microparticle is shown in Figure 2e. It was obvious that the γ-Fe_2O_3 MNPs and CdTe QDs with darker contrast were randomly embedded in the polymer matrix. The polyelectrolyte multilayer shell with brighter contrast could also be observed because the components of the polyelectrolytes had too low electron density to contribute to the contrast in the image.

(26) Yu, W. W.; Qu, L. H.; Guo, W. Z.; Peng, X. G. *Chem. Mater.* **2003**, *15*, 2854–2860.

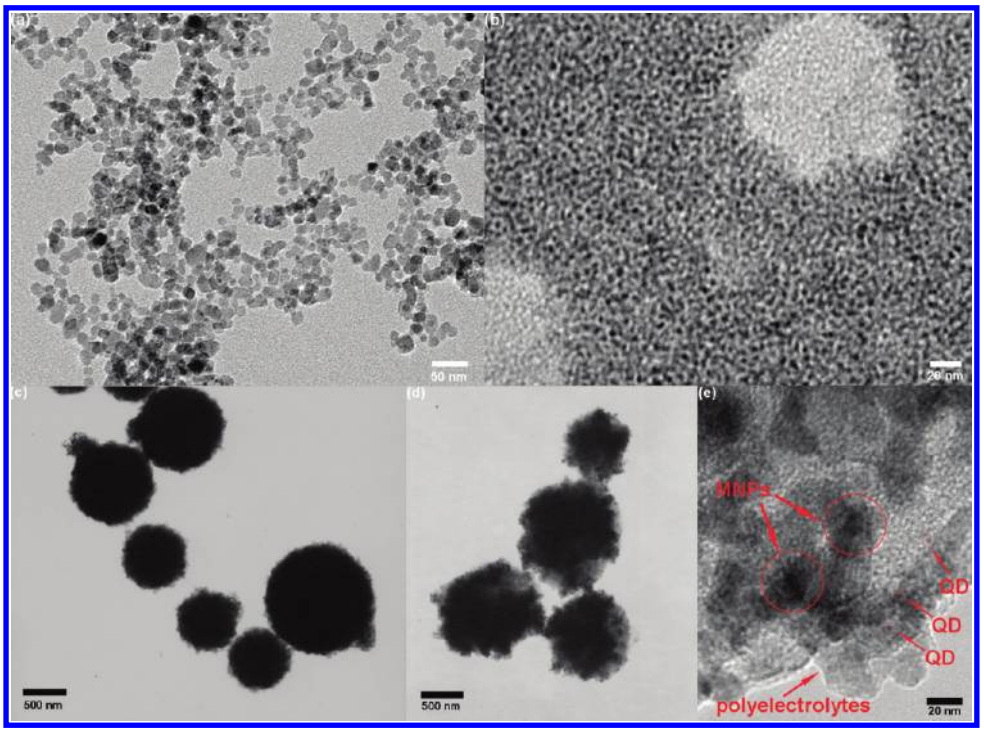

Figure 2. TEM images of (a) DMSA-coated γ-Fe_2O_3 MNPs, (b) MPA-capped CdTe QDs, (c) MAMs, (d) MAMs/$(PE_3/CdTe)_2$, and (e) an individual composite microparticle.

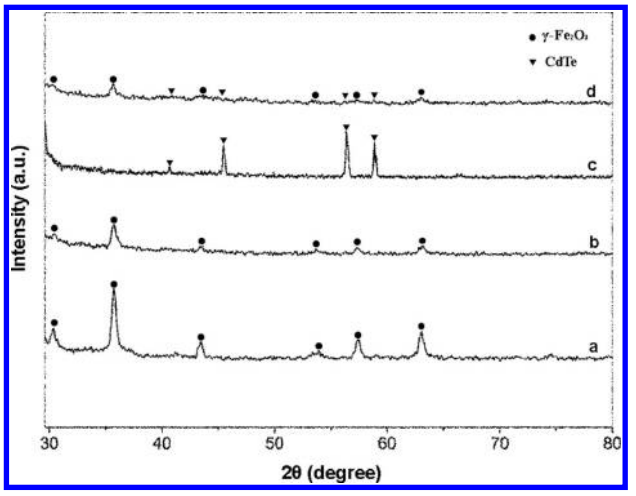

Figure 3. XRD patterns of (a) DMSA-coated γ-Fe_2O_3 MNPs, (b) MAMs, (c) MPA-capped CdTe QDs, and (d) MAMs/$(PE_3/CdTe)_2$.

XRD. XRD patterns of the as-synthesized products are shown in Figure 3. In Figure 3a, the position and relative intensity of main diffraction peaks matched well with standard maghemite (JCPDS no. 391346), indicating the inverse cubic spinel structure of the DMSA-coated γ-Fe_2O_3 MNPs. It is clearly seen from Figure 3b that the crystal structure of γ-Fe_2O_3 was well retained in the MAMs. As seen from Figure 3c, the XRD pattern shows several sharp diffraction peaks at the 2θ values of 45.8°, 56.3°, and 59.5° for CdTe in a hexagonal primitive-type structure (JCPDS no. 800090). The diffraction peak at the 2θ value of 41.6° possibly came from the CdS phase in a hexagonal primitive-type structure (JCPDS no. 430985). In the meantime, all peak positions and relative intensities of the MAMs/$(PE_3/CdTe)_2$ shown in Figure 3d were in good agreement with those of γ-Fe_2O_3 and CdTe crystals.

FTIR. Figure 4 represents the FTIR spectra of the DMSA-coated γ-Fe_2O_3 MNPs, sodium alginate, MAMs, MAMs/PE_7, MPA-capped CdTe QDs, and MAMs/PE_7/CdTe. It can be seen that the significant peaks for the γ-Fe_2O_3 MNPs (spectrum a) are at 635 and 568 cm^{-1}, attributed to the characteristic absorption bands of the Fe−O. The most significant peaks for alginate (spectrum b) at 1600 and 1410 cm^{-1} are attributed to carboxyl groups on alginate molecules. Spectrum c suggests a combining spectra of γ-Fe_2O_3 MNPs and alginate in the MAMs. The peaks at 1115 and 1170 cm^{-1} in spectrum d are attributed to the symmetric stretching vibration and asymmetric vibration of $-SO_3^-$ groups on PSS molecules, respectively, while the peak at 1470 cm^{-1} is attributed to $-NH_2$ groups on PAH molecules.[20] Spectrum d suggests a combining spectra of MAMs and PAH/PSS mixtures. The significant peaks for MPA-capped CdTe QDs (spectrum e) are at 1633 and 1416 cm^{-1}, attributed to carboxyl stretching vibration and methylene scissoring vibration of MPA molecules capped on the surface of CdTe QDs, respectively.[27] The broad peak at 1646 cm^{-1} in spectrum f can be assigned to imide, suggesting chemical complexation of cationic groups ($-NH_3^+$) of positively charged PAH and the negatively charged carboxyl groups ($-COO^-$) on the surface of the CdTe QDs.[28] These results indicate that the MAMs/PE_7/CdTe microparticles are composed of alginate, γ-Fe_2O_3 MNPs, PAH/PSS, and CdTe QDs.

PL. Figures 5a and 5b show the PL spectra of the MAMs/PE_n/CdTe (n = 3, 5, 7, 9) and MAMs/$(PE_3/CdTe)_n$ (n = 1, 2, 3, 4), which were measured at fixed concentration of MAMs, respectively. For both MAMs/PE_n/CdTe and MAMs/$(PE_3/CdTe)_n$, the peaks of PL spectra had a red shift of ~30 nm, and the PL intensity was enhanced with a corresponding increase of the polyelectrolyte multilayers and the CdTe QDs deposition cycles. The red shift of PL emission peak might be due to the interparticle interactions of adsorbed CdTe QDs on the composite microparicles. The PL intensity enhancement was probably attributed to the

(27) Wang, Y. Q.; Ye, C.; Zhu, Z. H.; Hu, Y. Z. *Anal. Chim. Acta* **2008**, *610*, 50–56.
(28) Yu, W. W.; Wang, Y. A.; Peng, X. G. *Chem. Mater.* **2003**, *15*, 4300–4308.

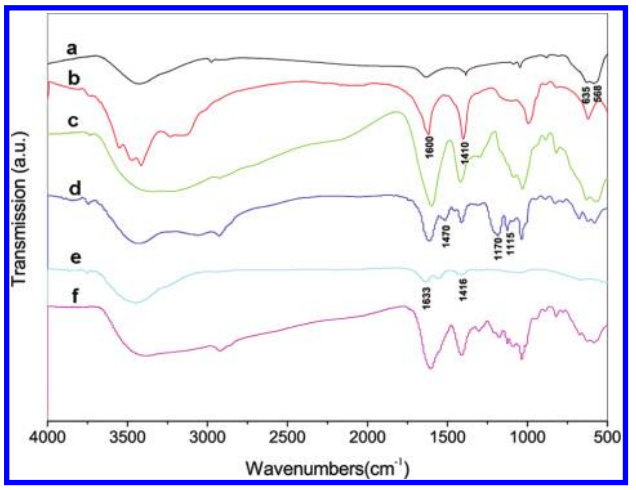

Figure 4. FTIR spectra of (a) DMSA-coated γ-Fe_2O_3 MNPs, (b) sodium alginate, (c) MAMs, (d) MAMs/PE_7, (e) MPA-capped CdTe QDs, and (f) MAMs/PE_7/CdTe.

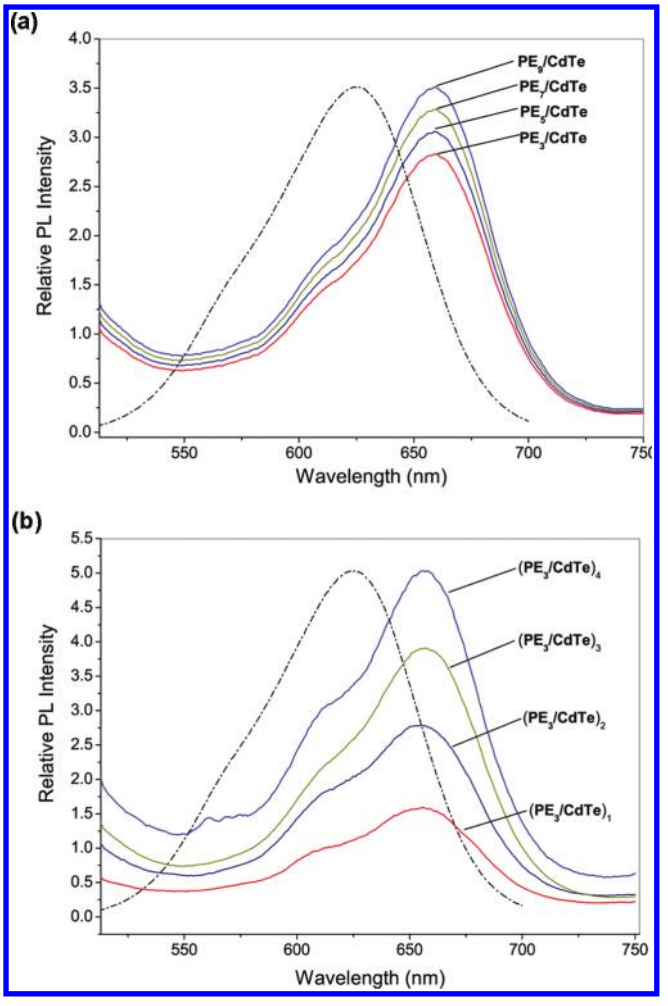

Figure 5. PL spectra of (a) MAMs/PE_n/CdTe (n = 3, 5, 7, 9) and (b) MAMs/$(PE_3/CdTe)_n$ (n = 1, 2, 3, 4). The dashed line show typical PL spectra of the pure CdTe QDs with emission peaks at 622 nm.

increasing surface area of a single microparticle with deposited polyelectrolyte multilayers, leading much more CdTe QDs to adsorb onto the surface of the microparticles. Another reason is that the interaction between the γ-Fe_2O_3 MNPs and CdTe QDs

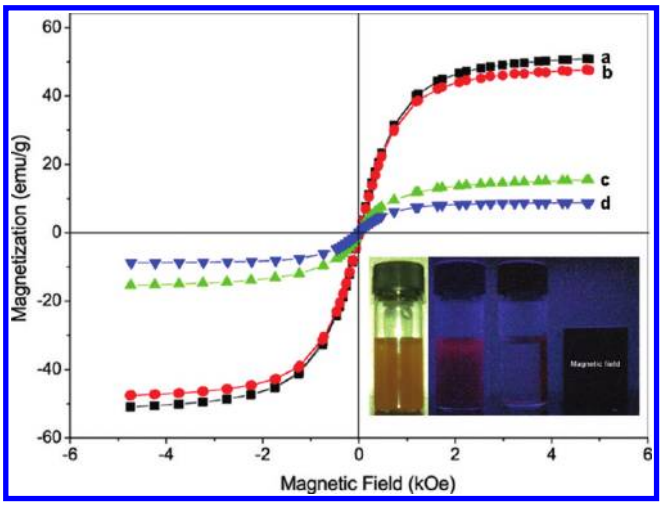

Figure 6. Room-temperature hysteresis loops of (a) uncoated γ-Fe_2O_3 MNPs, (b) DMSA-coated γ-Fe_2O_3 MNPs, (c) MAMs, and (d) MAMs/PE_7/CdTe. The inset shows photographic images of the composite microparticles under day light (left) and UV irradiation without (center) and with (right) an external magnetic field.

extremely sensitive to the separation distance, which lead to energy transfer and hence influence the PL properties, would be dramatically diminished with the increase of distance between the γ-Fe_2O_3 MNPs and CdTe QDs. Since the CdTe QDs were adsorbed on the surface of microparticles away from the γ-Fe_2O_3 MNPs, the PL might not be quenched significantly.[17] Moreover, the thickness of polyelectrolyte multilayers could be tuned to separate the γ-Fe_2O_3 MNPs and CdTe QDs. Thus, the PL intensity could be further increased by adjusting the polyelectrolyte multilayers and CdTe QDs deposition cycles.

Magnetization. Figure 6 shows the room-temperature hysteresis loops of the uncoated γ-Fe_2O_3 MNPs, DMSA-coated γ-Fe_2O_3 MNPs, MAMs, and MAMs/PE_7/CdTe. Magnetization measurements show that the alginate-templated composite microparticles maintained superparamagnetic nature contributed by the γ-Fe_2O_3 MNPs, as evidenced by the zero coercivity and the reversible hysteresis behavior at room temperature. The saturation magnetization (Ms) value of the MAMs (16.3 emu g^{-1}) was less than those of the DMSA-coated γ-Fe_2O_3 MNPs (47.7 emu g^{-1}) and uncoated γ-Fe_2O_3 MNPs (50.9 emu g^{-1}), which could be explained by nonmagnetic coating materials surrounding the magnetic cores. The magnetic content of the MAMs was estimated to be 32 wt %, which was consistent with the thermogravimetric analysis (TGA) result (see Figure S5 in the Supporting Information). After the polyelectrolyte multilayers and CdTe QDs were deposited on the surface of the MAMs, the Ms of the MAMs/PE_7/CdTe decreased to 9.7 emu g^{-1}, which was much higher than that in previously reported results.[15,16,18] Furthermore, the magnetic separability of these composite microparticles was tested by placing an external magnetic field, which in this case could be easily monitored through the intense luminescence of the microparticles. While in the absence of a magnetic field the dispersion of the composite microparticles was red and homogeneous under UV radiation (see inset in Figure 6, center). When the external magnetic field (Nd−Fe−B magnet, 0.5 T) was applied, the microparticles were attracted toward the magnet within 10 s, and the dispersion became clear and transparent (see the inset in Figure 6, right). With removal of the magnetic field followed by stirring, the aggregations were rapidly redispersed. This will allow for an easy and efficient way to separate the composite microparticles from a suspension system under an external magnetic field.

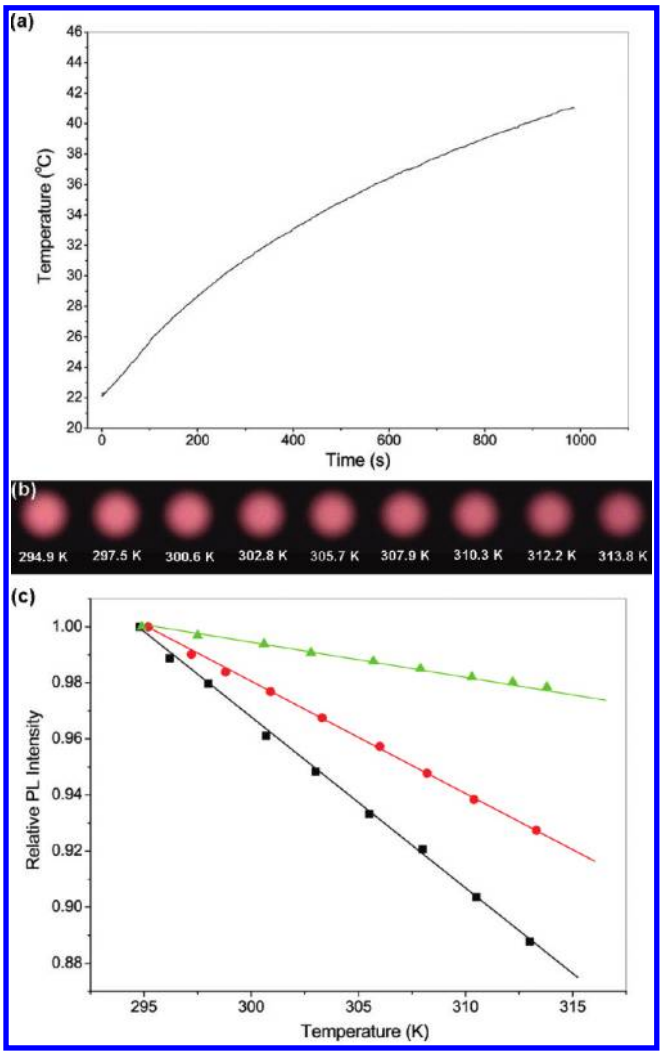

Figure 7. (a) Temperature increase curve of MAMs/PE_7/CdTe when applying the HFMF. (b) Fluorescent images of MAMs/PE_7/CdTe at different temperatures. (c) PL intensity of CdTe QDs (black squares), MAMs/PE_7/CdTe (red circles), and MAMs/PE_7/CdTe/$(PAH/PSS)_3$ (green triangles) as a function of temperature.

Temperature-Dependent PL under HFMF. Because of the inductive effect of the γ-Fe_2O_3 MNPs in the presence of HFMF,[29,30] temperature for the MAMs/PE_7/CdTe increased to 314 K under HFMF treatment for 15 min (Figure 7a). As shown in Figure 7b, the PL intensity declined with increasing temperature over the range from 294.9 to 313.8 K. The decline of PL intensity is caused by the thermal activation of surface traps leading to nonradiative recombination of excitons.[31] Red-shifted PL characteristics were also observed and accounted for a quantum mechanical tunneling through interdot barriers or thermal excitation followed by hopping above the energy barrier due to interdot exciton coupling[32] (see Figure S6 in the Supporting Information). It was possible to estimate that the PL intensity of the MAMs/PE_7/CdTe decreased linearly ($\sim$0.39% K^{-1}) with increasing temperature compared to that of pure CdTe QDs ($\sim$0.61% K^{-1}). When three bilayers $(PAH/PSS)_3$ were combined to the CdTe QDs on the surface of the MAMs/PE_7/CdTe, the PL intensity decreased with a rate of $\sim$0.11% K^{-1} (Figure 7c). It is reported that the modification of QDs surface is important for the PL sensitivity to the temperature.[33] Therefore, the desired selectivity could be controlled by chemically tailoring the outer surface of the adsorbed CdTe QDs.

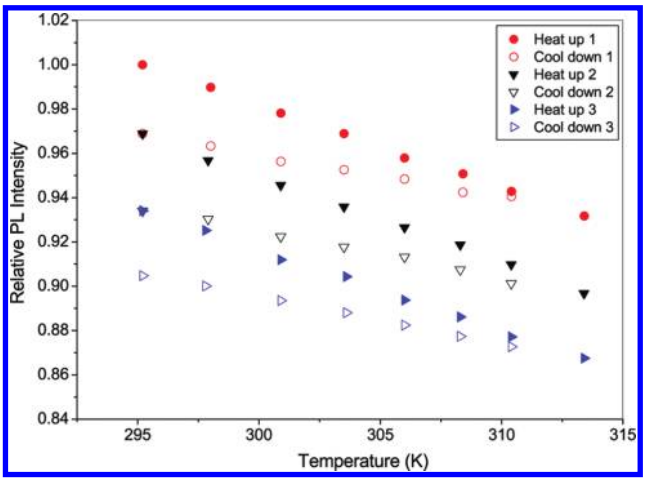

Figure 8. PL intensity of MAMs/PE_7/CdTe as a function of temperature during three heat-up and cool-down cycles.

The PL intensity of the MAMs/PE_7/CdTe was linearly and reversibly proportional to the temperature between 295.2 and 313.4 K in heating−cooling cycles (Figure 8). However, the PL intensity obtained in the cooling is a little lower than its original in the heating. Possible explanation for this could be that some reactions such as oxidation would occur, which disturbed the repopulation of mobile electrons and holes leading to the irreversible PL quenching.[11,13] Another reason might be that ionically cross-linked alginate gels may dissolve due to the loss of cross-linking Ca^{2+} in repetitive heating process, which might lead to the release of γ-Fe_2O_3 MNPs or CdTe QDs from the composite microparticles. Therefore, the stability of the composite microparticles in the presence of HFMF was investigated. TEM and SEM images of the MAMs/PE_7/CdTe after three heat-up and cool-down processes are shown in Figure S7 of the Supporting Information. It can be seen that the particles are largely spherical, and no free γ-Fe_2O_3 MNPs and CdTe QDs are observed outside the microparticles. Inductive coupled plasma emission spectrometry (ICP) was also carried out to check the release of γ-Fe_2O_3 MNPs or CdTe QDs from the composite microparticles. No Fe^{3+}, Ca^{2+}, or Cd^{2+} was detected in the supernatant of the composite microparticles after several heating processes, demonstrating that no γ-Fe_2O_3 MNPs or CdTe QDs were released from the composite microparticles. This result was consistent with the results from TEM and SEM imaging. The as-synthesized alginate-templated composite microparticles can possess excellent magnetic and luminescent functionalities and favorable stability in the presence of HFMF, which are particularly interesting in biological or biomedical applications, such as *in vitro* and *in vivo* thermometry during hyperthermia treatment.

Conclusions

The dual-functional (magnetic/luminescent) alginate-templated composite microparticles were successfully synthesized by a novel process combining the emulsification and layer-by-layer self-assembly techniques. The composite microparticles had excellent

(29) Sun, Y. K.; Ma, M.; Zhang, Y.; Gu, N. *Colloids Surf., A* **2004**, *245*, 15–19.
(30) Xu, R. Z.; Zhang, Y.; Ma, M.; Xia, J. G.; Liu, J. W.; Guo, Q. Z.; Gu, N. *IEEE Trans. Magn.* **2007**, *43*, 1078–1085.
(31) Biju, V.; Makita, Y.; Sonoda, A.; Yokoyama, H.; Baba, Y.; Ishikawa, M. *J. Phys. Chem. B* **2005**, *109*, 13899–13905.
(32) Kim, B. S.; Islam, M. A.; Brus, L. E.; Herman, I. P. *J. Appl. Phys.* **2001**, *89*, 8127–8140.
(33) Wang, J. H.; Wang, H. Q.; Li, Y. Q.; Zhang, H. L.; Li, X. Q.; Hua, X. F.; Cao, Y. C.; Huang, Z. L.; Zhao, Y. D. *Talanta* **2008**, *74*, 724–729.

magnetic properties, and its photoluminescence could be precisely controlled by varying the number of deposition cycles of polyelectrolytes and CdTe/polyelectrolyte multilayers. In addition, the composite microparticles could be heated up in high-frequency magnetic field and demonstrated linear temperature-dependent photoluminescence over the range from room temperature to hyperthermia temperature. By further modification of the adsorbed CdTe QDs on the microparticles, different temperature-sensitive composite microparticles could be obtained. These composite microparticles with magnetic and luminescent functionalities could serve both as magnetic materials for hyperthermia and as optical temperature probes for temperature monitoring during hyperthermia treatment. Better strategies are also needed to develop multifunctional nanoparticle systems and optimize the material behavior, i.e., synthesis of high-quality magnetic nanoparticles for magnetic induction hyperthermia and luminescent nanoparticles with excellent signal reproducibility and sensitivity for thermometry. It is believed that these composite microparticles could be derivatized to bind to targeted agents such as proteins or antibodies, which may have potential applications in cancer diagnosis and treatment.

Acknowledgment. This work was supported by National Natural Science Foundation of China (Nos. 30870679, 50872021, and 90406023), National Basic Research Program of China (Nos. 2011CB933503, 2006CB933206, and 2006CB705606), and Qing Lan Project.

Supporting Information Available: Schematic diagram of detection system, UV−vis absorption and PL spectra of MPA-capped CdTe QDs, SEM images of MAMs and MAMs/$(PE_3/CdTe)_2$, EDS data from MAMs/$(PE_3/CdTe)_2$, TGA curve of MAMs, PL spectra of MAMs/PE_7/CdTe at different temperatures, TEM and SEM images of MAMs/PE_7/CdTe after three heat-up and cool-down processes. The material is available free of charge via the Internet at http://pubs.acs.org.